The Lymphocyte-specific Protein LSP1 Binds to F-actin and to the Cytoskeleton Through Its COOH-terminal Basic Domain

J. Jongstra-Bilen,* P. A. Janmey,‡ J. H. Hartwig,‡ S. Galea,* and J. Jongstra*

*Department of Immunology, University of Toronto and the Toronto Western Hospital, Toronto, Ontario M5T 2S8, Canada; and ‡Experimental Medicine Division, Brigham and Women's Hospital, Harvard Medical School, Boston, Massachusetts 02115

Abstract. The lymphocyte-specific phosphoprotein LSP1 associates with the cytoplasmic face of the plasma membrane and with the cytoskeleton. Mouse LSP1 protein contains 330 amino acids and contains an NH_2-terminal acidic domain of ~177 amino acids. The COOH-terminal half of the LSP1 protein is rich in basic residues. In this paper we show that LSP1 protein which is immunoprecipitated with anti-LSP1 antibodies from NP-40–soluble lysates of the mouse B-lymphoma cell line BAL17 is associated with actin. In vitro binding experiments using recombinant LSP1 (rLSP1) protein and rabbit skeletal muscle actin show that LSP1 binds along the sides of F-actin but does not bind to G-actin. rLSP1 does not alter the initial polymerization kinetics of actin. The highly conserved COOH-terminal basic domains of mouse and human LSP1 share a significant homology with the 20-kD COOH-terminal F-actin binding fragment of caldesmon. A truncated rLSP1 protein containing the entire COOH-terminal basic domain from residue 179 to 330, but not the NH_2-terminal acidic domain binds to F-actin at least as well as rLSP1. When LSP1/CAT fusion proteins are expressed in a LSP1-negative T-lymphoma cell line, only fusion proteins containing the basic COOH-terminal domain associate with the NP-40–insoluble cytoskeleton. These data show that LSP1 binds F-actin through its COOH-terminal basic domain and strongly suggest that LSP1 interacts with the cytoskeleton by direct binding to F-actin. We propose that LSP1 plays a role in mediating cytoskeleton driven responses in lymphocytes such as receptor capping, cell motility, or cell–cell interactions.

LSP1 is a lymphocyte-specific intracellular Ca^{2+}-binding phosphoprotein (18–20). LSP1 protein contains an acidic NH_2-terminal and a basic COOH-terminal domain, the latter being highly conserved between the mouse and the human predicted amino acid sequences (19). In the mouse B-lymphoma cell line BAL17, LSP1 is distributed in three different subcellular fractions. ~25% of total cellular LSP1 associates with the cytoplasmic face of the plasma membrane, 10–20% with the cytoskeleton, and the rest partitions to soluble cytoplasm (20, 21). Activation of B-lymphoma cell lines by cross-linking of their membrane immunoglobulin (mIg)[1] molecules with anti-Ig antibodies results in the aggregation of LSP1 directly under the extracellular caps formed by cross-linked mIgM molecules (21). This localization of LSP1 beneath caps, and its association with both lymphocyte membrane and cytoskeleton, implicates LSP1 in the cytoskeletal remodeling after B-cell activation.

Normal resting B-lymphocytes which express mIg molecules on the surface as antigen receptors undergo a transition from the G_0 to G_1 stage after treatment with anti-Ig antibodies (10, 40). Some of the biochemical changes in the cell after activation of resting B-cells or B-lymphoma lines with antigen or anti-Ig include a rapid activation of phosphotyrosine kinase activity (8, 12, 32), and an activation of the phosphatidylinositol pathway (3, 9, 31). Moreover, the intracellular free Ca^{2+} increases rapidly and transiently within seconds after anti-Ig stimulation (36, 37). In addition to these biochemical changes, dramatic structural changes occur in activated B-cells as well. These include the rapid association of a fraction of mIg molecules with the cytoskeleton (1, 5, 45), a rapid increase in polymerized F-actin (29), patching, capping, and endocytosis of mIg molecules (4) and a rapid and transient stimulation of cell motility (39). Eventually all or part of these biochemical and structural changes cooperate with signals delivered by lymphokines such as IL-4 to initiate new DNA synthesis and cell growth (17) and it has become apparent that the cytoskeleton plays a central role in the transmission of these mitogenic signals (1, 14, 29, 38).

To determine how LSP1 protein might be involved in the regulation of cytoskeletal structure we investigated if LSP1 interacts with other cellular proteins. Using immunoprecipitations, direct binding studies and EM, we show that LSP1 is an F-actin binding protein which binds to the sides of actin filaments. The COOH-terminal basic domain of LSP1 binds

1. *Abbreviations used in this paper*: CAT, chloramphenicol acetyl transferase; mIg, membrane immunoglobulin; OGP, 1-0-n-octyl-b-D-glucopyranosid; rLSP1, recombinant LSP1.

to F-actin in vitro while the same domain also binds to the cytoskeleton in intact cells. This suggests that the cytoskeletal localization of LSP1 is due to its binding to F-actin.

Materials and Methods

Cells and Antisera

The mouse mIgM$^+$, and mIgD$^+$ B-lymphoma line BAL17, mIgM$^+$ B-lymphoma line WEHI231, and T-lymphoma line BW5147 were grown in complete RPMI-1640 tissue culture medium supplemented with 10% FCS as described (20). T22 is a clonal derivative of the LSP1$^+$ BW5147 transfectant no. 2 (20). The anti-LSP1 serum was made in rabbits against the mouse recombinant LSP1 protein (rLSP1) (20). LSP1-specific affinity purified antibodies were isolated by passing this serum through a column of rLSP1 coupled to CNBr-activated Sepharose. The monoclonal anti-actin antibody 14.3 was supplied as a hybridoma supernatant and was a gift from Dr. Dominique Aunis (Centre de Neurochimie, Strasbourg, France). Polyclonal rabbit anti-chloramphenicol acetyl transferase (CAT) antiserum was purchased from 5'-3', Inc. (Boulder, CO).

Immunoprecipitations

BAL17 cells (10^6 cells/ml) were washed once with prewarmed HBSS and were labeled for 16 h in 90% methionine-free and 10% complete culture medium (1% final FCS) containing 10 μCi/ml [^{35}S]methionine (Translabel, 1,000 Ci/mmol; ICN K&K Laboratories Inc., Plainview, NY). After labeling, the cells were washed twice with HBSS and lysed at a concentration of 10^7 cells/ml in a lysis buffer containing 50 mM Tris-HCl, pH 7.2, 150 mM NaCl, 1 mM $MgCl_2$, 0.5% NP-40, 14 μg/ml aprotinin, 1 mM PMSF, 2 μg/ml leupeptin, 1 μg/ml pepstatin A, and either 2 mM EGTA or 100 μM $CaCl_2$, as indicated. Immunoprecipitations were performed as described previously (30) using affinity-purified anti-LSP1 antibodies, total anti-LSP1 serum, or normal rabbit serum. Protein A-Sepharose beads (Sigma Chemical Co., St. Louis, MO) were prepared in lysis buffer as 1:1 slurry and 15 μl of this slurry was added to lysates corresponding to 3×10^6 cells. The beads were washed three times with RIPA (radioimmunoprecipitation assay) buffer (50 mM Tris-HCl, pH 7.2, 150 mM NaCl, 1 mM $MgCl_2$, 1% NP-40, 0.5% deoxycholate, 0.1% SDS, and either 2 mM EGTA or 100 μM Ca^{2+}) and once with TBS, pH 7.2, containing either 2 mM EGTA or 100 μM Ca^{2+}. The immunecomplexes were collected from the beads by addition of 50 μl Laemmli sample buffer (25) and immersion in boiling water for 5 min followed by centrifugation in a microfuge for 5 min. The immunecomplexes from 3×10^6 cells were analyzed on a SDS-10% acrylamide gel by fluorography.

Western Blot Analyses

Protein samples were separated on SDS-10% polyacrylamide gels and Western blot analysis was performed on Immobilon membranes (Millipore Corp., Bedford, MA) using the Bio-Rad Immunblot Assay Kit (Bio-Rad Laboratories, Richmond, CA) as described (20).

Rabbit Skeletal Muscle G-actin

Rabbit skeletal muscle F-actin (42) was dialyzed extensively against G-buffer (2 mM Tris-HCl, pH 7.6, 0.2 mM ATP, 0.2 mM DTT, and 0.2 mM $CaCl_2$). G-actin thus obtained was centrifuged in a Beckman airfuge (Beckman Instruments, Inc., Fullerton, CA) (28 psi, 1 h) to eliminate the remaining filaments and was stored on ice for use within 1 wk.

Preparation of DNAaseI-Sepharose Beads

DNAaseI from bovine pancreas (grade I, Boehringer Mannheim Corp., Montreal, Quebec) was coupled to CNBr-activated Sepharose beads (Sigma Chemical Co.) according to the Pharmacia Fine Chemicals (Piscataway, NJ) manual. The coupling was performed by incubation overnight at 4°C. Beads were stored at 4°C in 50 mM Tris-HCl, pH 7.2, 0.5 mM $CaCl_2$, and 0.01% methiolate as 1:1 slurry.

Preparation of NP-40 Soluble Lysates for Binding to the DNAaseI-Sepharose Beads

Cell lysates were prepared as described above using a slightly modified lysis buffer which contained 20 mM Tris-HCl, pH 7.2, 100 mM NaCl, 0.4% NP-40, and 2 mM EGTA with protease inhibitors as indicated above. ATP and DTT were added to the lysates to final concentrations of 0.2 mM. DNAaseI-Sepharose beads (200 μl 1:1 slurry) were equilibrated by washing five times with the above buffer containing 0.2 mM ATP and 0.2 mM DTT before incubating with 1 ml lysate (10^7 cells) for 15 min at room temperature with end-over-end mixing. The beads were then spun at 13,000 rpm for 2 min and the supernatants were collected. To analyze the material bound to the DNAase I beads, beads were washed five times with the above buffer containing ATP and DTT and boiled in 250 μl Laemmli sample buffer.

F-actin Binding Assay and Scatchard Plot Analyses

Proteins in P-buffer (10 mM imidazole, pH 7.0, 75 mM KCl, 0.2 mM DTT, 0.2 mM EGTA, 0.01% NP-40) were prespun in an airfuge (28 psi, 1 h) and mixed with G-actin. Control samples were mixed with an equivalent amount of G-buffer. Assays were performed in P-buffer containing 2 mM $MgCl_2$ and 0.1 mM ATP in a final volume of 100 μl. After incubation for 45 min at room temperature the samples were spun in an Airfuge (28 psi, 1 h). Laemmli sample buffer was added to both supernatants and pellets which were analyzed by SDS-PAGE and Coomassie staining. For Scatchard plot analyses, stained gels were scanned with a Hewlett Packard ScanJetPlus instrument (Mountain View, CA) and the density of each LSP1 and actin band was measured using the integrated density function of Image software version 1.29 (National Institutes of Health, Bethesda, MD). Each gel containing either pellets or supernatants from sedimentation assays also contained a series of lanes with known amounts of both actin and LSP1 spanning the range of amounts expected for the samples to be measured. For each gel, a calibration curve was constructed by plotting the density of the actin and LSP1 bands versus amounts of actin or LSP1 determined by optical density measurements at 290 and 280 nm, respectively, using extinction coefficient of 25800 $mol^{-1}cm^{-1}$ for actin and 34560 $mol^{-1}cm^{-1}$ for LSP1. The amount of protein in unknown samples was then calculated from a linear fit to the calibration curve. The amount of LSP1 bound to actin was taken from the ratio of LSP1 to actin in each pellet and is expressed in molar terms relative to sedimented actin. The amount of LSP1 remaining in the supernatant is taken as representing free LSP1.

Fluorescence and Light-Scattering Measurements

Fluorescence and light scattering at 90°C during the polymerization of pyrene-labeled actin were measured simultaneously in a Perkin-Elmer LS-50 instrument (The Perkin-Elmer Corp., Norwalk, CT) using the Intracellular Biochemistry setting which allows rapidly alternating measurements of light emitted at two wavelengths. The exciting wavelength was set at 365 nm, within the excitation peak of the pyrene label, and the emission wavelength alternated between 386 nm to measure fluorescence and 365 nm for scattering. The slit widths were set to 2.5 nm for both emission and excitation, and the period between two successive fluorescence or scattering measurements was 1.1 s. 3 μM pyrene-labeled G-actin was added to 300 μl PO buffer or to PO buffer containing either 3.5 μM LSP1 or 0.06 μM gelsolin and 200 μM $CaCl_2$. PO buffer is similar to P buffer except it contains 7.5 mM 1-0-n-octyl-b-D-glucopyranosid (OGP) (Boehringer Mannheim Corp.) instead of 0.01% NP-40. Polymerization was initiated by adding 0.2 mM ATP and 2.0 mM $MgCl_2$ immediately after addition of G-actin.

Electron Microscopy

Negative staining of actin filaments with or without rLSP1 or the 5-1 fusion protein was performed using 2% uranyl acetate. Purified rLSP1 and 5-1 proteins were visualized by rotary shadowing with tantalum-tungsten at 5°. Proteins in 50% glycerol were sprayed onto mica, dried in a vacuum, and metal coated (43).

Expression of LSP1/CAT Fusion Proteins and Truncated Fusion Proteins

The cDNA insert of pJJ32 (18) was excised with EcoRI and transferred to the EcoRI site of the Bluescript plasmid vector such that the 5' end of the cDNA was close to the PstI site in the Bluescript polylinker. After digestion with ClaI and religation, the Bluescript vector contained the LSP1 translation initiation codon followed by five NH_2-terminal LSP1 amino acid residues (pBS/LSP1-ATG). The pBS/LSP1-ATG plasmid was cut with SalI and XhoI and a CAT cassette with SalI linkers at both ends encoding the chloramphenicol transferase enzyme, CAT (Pharmacia Fine Chemicals) was in-

serted in such a way that LSP1 and CAT proteins were read in the same orientation to give pBS/LSP1-ATG/CAT. In a final step the ApaI site in the polylinker of this plasmid was converted to a BamHI site using a BamHI linker. This allowed us to excise the LSP1/CAT sequences as a BamHI fragment. The 711 expression vector was then constructed by transferring the BamHI fragment of pBS/LSP1-ATG/CAT to the unique BamHI site of the eukaryotic expression vector pBJ1-neo (27), which had been modified as follows. The unique XhoI site in pBJ1-neo was converted to a BamHI site by insertion of a linker sequence, the resulting plasmid was cut with BamHI and religated resulting in the deletion of all polylinker sequences. After ensuring that the translation initiation codons of LSP1 and CAT were in the same reading frame by sequencing we transfected the 711 vector into the T-lymphoma line BW5147 and selected a stably transfected G418 (Geneticin, Gibco Laboratories, Grand Island, NY) resistant cell line, BW711 (see Fig. 8). The fusion protein expressed in BW711 consists of six NH_2-terminal LSP1 amino acids followed by 16 residues encoded by the pBS polylinker and the CAT 5′ untranslated region followed by the 219-amino acid residue CAT protein. Other LSP1/CAT fusion proteins (see Fig. 8 for a schematic representation) were expressed after cloning the appropriate fragments of LSP1 cDNA in ClaI/SalI cut 711 vector and all contain the six NH_2-terminal LSP1 amino acids and 14 residues encoded by the pBS polylinker and the CAT 5′ untranslated region. LSP1 fragments were isolated by PCR amplification using pJJ32 as a template with forward primers containing a ClaI recognition site and reverse primers containing a SalI recognition site at their 5′ end.

To express 5-1a and 6-1a recombinant proteins the BamHI fragment containing the LSP1/CAT fusion construct used to establish cell lines BW57 (for 5-1a) and BW71 (for 6-1a) were transferred to pBS and a frame shift mutation was introduced at the SalI site resulting in the translation of 12 amino acids of the vector sequences between LSP1 and CAT after which the reading frame is interrupted by a translational stop codon. Thus 5-1a protein contains the complete acidic domain of LSP1 (residues 1–178) followed by 12 vector derived residues, while 6-1a protein contains the first six NH_2-terminal LSP1 residues followed by the complete LSP1 basic domain (residues 179–330) and the 12 vector derived amino acids. After transfer of the BamHI fragments to the prokaryotic expression vector pET-3c the 5-1a and 6-1a proteins were expressed and purified as described below. To prepare 5-1 recombinant protein the A-CAT insert (see Fig. 8) was subcloned into the pET-3c vector and the protein was purified as described below. All recombinant proteins expressed from the pET-3c vector contain 11 identical vector derived amino acid residues at their NH_2 terminus (20).

Purification of Recombinant Proteins

The purification was performed essentially as described (20) except that after removal of SDS the samples were further dialyzed against P buffer containing 0.01% NP-40. Protein samples were concentrated using a Centriprep-10 concentrator (Amicon, Beverly, MA).

Determination of LSP1 and LSP1/CAT Fusion Proteins in the Cytoskeletal Fractions

Cytoskeletal fractions were obtained as described (21, 34) by lysis of cells in an NP-40-containing buffer and low-speed centrifugation for 10 min at 600 *g*. The amount of wild-type LSP1 or LSP1/CAT fusion proteins in the cytoskeletal fractions was determined by Western blotting as a percentage of that present in a total cell lysate prepared by lysing cells in SDS containing Laemmli buffer. This was done as described (21) by comparing the LSP1 signal in a series of twofold dilutions of the NP-40 insoluble pellets to the signal in a constant amount of total cell lysate. The ratio of cell equivalents of NP-40-insoluble pellet and total cell lysate needed to obtain equal signals was used to calculate the percentage of LSP1 protein in the NP-40-insoluble pellet.

Results

Previously we have commented on the lack of significant sequence homology between the predicted amino acid sequence of LSP1 and sequences in the GenBank and NBRF databases (18, 19). However, as shown in Fig. 1, a search of updated databases revealed a 46% homology (34% identical amino acids and 12% chemically conserved substitutions) between the 20-kD COOH-terminal actin binding fragment

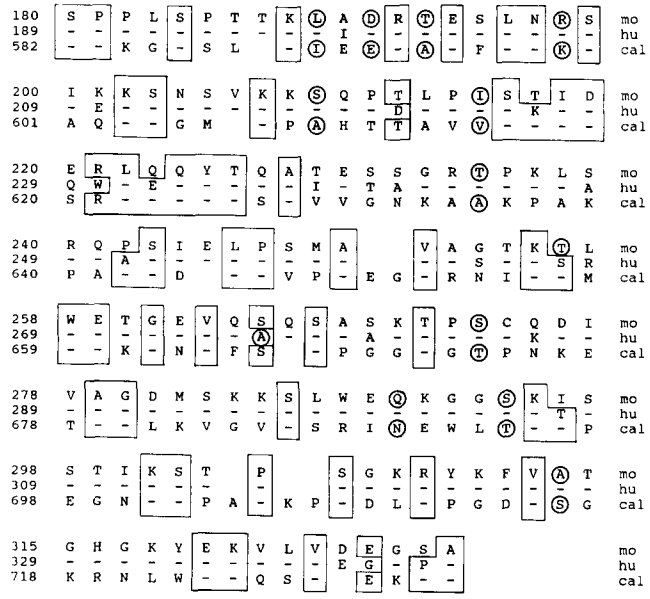

Figure 1. Comparison of the predicted protein sequences of the basic domains of the mouse and human LSP1 proteins with the sequence of the COOH-terminal F-actin binding fragment of caldesmon. The abbreviations mo, hu, and cal on the right indicate mouse LSP1, human LSP1, and chicken caldesmon, respectively. Gaps are introduced for optimal alignment. (−) Residues identical with those directly above. Boxes indicate identical amino acids in either one or both of the LSP1 proteins and caldesmon. Chemically conserved substitutions are circled. Numbers on the left correspond to amino acid positions starting at the NH_2 terminus of the protein sequences. These sequence data are available from GenBank under accession number M33552 (huLSP1) and from NBRF under accession numbers A30533 (moLSP1) and A32642 (cal).

of chicken smooth muscle caldesmon (6) and the highly conserved COOH-terminal basic domains of mouse and human LSP1 protein (19). This sequence spans 152 amino acid residues and includes homology to regions of caldesmon which are required for binding to F-actin (44). This sequence homology, and the finding that up to 20% of LSP1 is cytoskeletal in lymphocytes prompted us to determine if LSP1 binds actin, and since LSP1 binds Ca^{2+} (20) we asked whether such an interaction would be modulated by Ca^{2+}.

LSP1 Interacts with Actin in BAL17 Lysates

To determine whether the intracellular protein LSP1 is associated with actin we immunoprecipitated the LSP1 protein from the mouse $sIgM^+$, $sIgD^+$ B-lymphoma cell line BAL17 in the presence of Ca^{2+} or EGTA. Fig. 2 *a* illustrates a typical result of such an immunoprecipitation. In addition to the 52-kD band which was identified as a product of the LSP1 gene (indicated by an *open arrowhead* in Fig. 2) (20), a prominent 42-kD protein (p42, indicated by a *closed arrowhead* in Fig. 2) was present in the presence of either 2 mM EGTA (Fig. 2 *a*, lane *1*) or 100 μM Ca^{2+} (Fig. 2 *a*, lane *2*). Fig. 2 *a* also shows that immunoprecipitates formed with normal rabbit serum did not contain the LSP1 or p42 proteins either in the absence (Fig. 2 *a*, lane *3*) or presence (Fig. 2 *a*, lane *4*) of Ca^{2+}. The nature of the 90-kD band present in Fig. 2 *a*, lanes *1* and *2* is as yet unknown.

To determine whether the presence of p42 in our immunoprecipitates is due to a cross-reaction of the anti-LSP1 serum with p42, immunoprecipitations were performed from the transformed T-cell line BW5147 which does not ex-

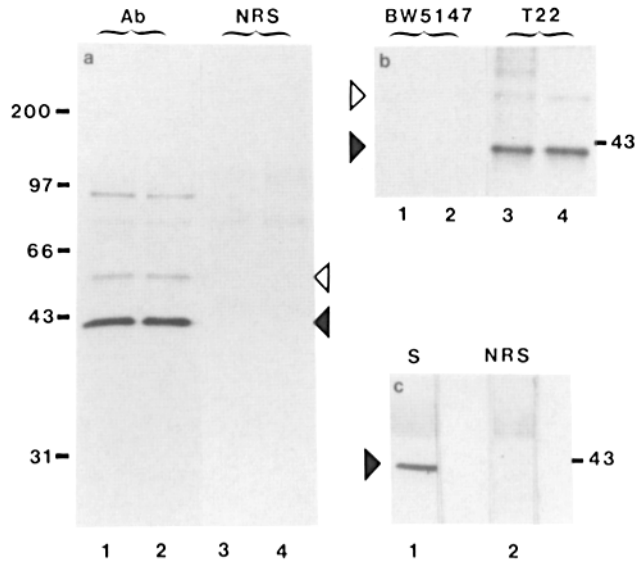

Figure 2. LSP1 binds to actin. (*a*) Immunoprecipitations were performed in the presence of 2 mM EGTA (lanes *1* and *3*) or 100 μM Ca^{2+} (lanes *2* and *4*) with affinity purified anti-LSP1 antibodies (*Ab*, lanes *1* and *2*) or with pre-immune normal rabbit serum (*NRS*, lanes *3* and *4*) at 1:500 and 1:200 dilutions, respectively. The open arrowhead indicates the position of the 52-kD LSP1 protein while the closed arrowhead indicates the position of purified rabbit skeletal muscle actin used as a marker protein. The numbers to the left correspond to the positions of marker proteins with their molecular mass indicated in kilodaltons. (*b*) Immunoprecipitates of $LSP1^-$ T-cell line BW5147 (lanes *1* and *2*) and its $LSP1^+$ derivative T22 (lanes *3* and *4*) after lysis in the presence of either 2 mM EGTA (lanes *1* and *3*) or 100 μM Ca^{2+} (lanes *2* and *4*). The positions of LSP1 and of the actin marker are indicated with an open and closed arrowhead at the left. (*c*) Immunoprecipitations performed with anti-LSP1 serum (*S*, lane *1*) or normal rabbit serum (*NRS*, lane *2*) at 1:200 dilutions were analyzed by Western blotting using mAb against rabbit skeletal muscle actin at a dilution of 1:10. The position of purified rabbit skeletal muscle actin is indicated with an arrow to the left.

press LSP1 protein and from its $LSP1^+$ derivative T22, established by transfection with LSP1 cDNA in the expression vector pECE-B (20). Fig. 2 *b* shows that no p42 or LSP1 were present in immunoprecipitates from BW5147 cell lysates made in 2 mM EGTA or 100 μM Ca^{2+} (Fig. 2 *b*, lanes *1* and *2*), while both p42 and LSP1 were precipitated from such lysates of the $LSP1^+$ T22 transfectant (Fig. 2 *b*, lanes 3 and 4). These results show that p42 is present in BW5147 cell lysates but is only precipitated with anti-LSP1 antibodies when LSP1 protein is present as well. We conclude from these data that p42 and LSP1 form a protein complex in the cell lysate in a Ca^{2+}-independent manner.

Based on its molecular weight and on its comigration with purified actin in NEPHGE/SDS-10% acrylamide two-dimensional gels (not shown) we predicted p42 to be actin. To verify this point we analyzed [^{35}S]methionine-labeled anti-LSP1 immunoprecipitates by Western blotting using mAbs against rabbit skeletal muscle actin (Fig. 2 *c*). This mAb identified p42 as actin only in the anti-LSP1 immunoprecipitate (Fig. 2 *c*, lane *1*) but not in the precipitate formed with pre-immune rabbit serum (Fig. 2 *c*, lane *2*), identical to the pattern obtained by autoradiography of the Western blot (not shown). These data confirm that actin is the [^{35}S]methionine-labeled p42 shown in Fig. 2 *a* to interact with LSP1.

LSP1 Binds to F-actin but not to G-actin

Control experiments established that rLSP1 is not soluble under conditions of actin polymerization unless some NP-40 detergent was added. We therefore routinely added 0.01% NP-40 to all our F-actin binding assays. Fig. 3 *a*, lanes *1–3* show that rLSP1 is soluble in the presence of 0.01% NP-40 when incubated in the absence of actin. However, upon addition of G-actin and after polymerization, a significant portion of added rLSP1 cosediments with F-actin (Fig. 3 *a*, lane *5*) while a small fraction remains in the supernatant (Fig. 3 *a*, lane *4*). LSP1 does not affect the amount of F-actin sedimenting in this assay system (compare Fig. 3 *a*, lanes *4* and *5* with lanes *6* and *7*). The binding of rLSP1 to F-actin was not affected by the addition of 0.1 mM Ca^{2+} or 0.2 M NaCl to the assay media (data not shown). The same results were obtained when LSP1 from actin depleted NP-40 soluble BAL17 lysates was used as a source of native LSP1 to bind to F-actin in vitro (not shown). Fig. 3 *b* illustrates a specificity control with BSA. Whether incubated under polymerization conditions in the absence (Fig. 3 *b*, lanes *1* and *2*) or presence (Fig. 3 *b*, lanes *3* and *4*) of actin all of the BSA remains in the supernatant fractions as soluble protein. We conclude from these in vitro actin-binding assays that LSP1 protein binds to F-actin in a Ca^{2+}-independent manner.

To check whether the basic domain of LSP1, which contains the homology with the F-actin binding domain of caldesmon (see Fig. 1), binds to F-actin we performed similar experiments with the truncated LSP1 recombinant protein, 6-la, which contains the entire basic domain of LSP1. Fig. 3 *c* shows that while the 6-la protein is soluble in the absence of actin (Fig. 3 *c*, lanes *1* and *2*), most of this protein coprecipitates with F-actin (Fig. 3 *c*, lanes *3* and *4*). The same assay was also performed with another truncated LSP1 protein, 5-la, which contains the entire acidic NH_2-terminal domain of LSP1 and the same additional amino acids from the vector as for 6-la (see Materials and Methods). This protein did not bind to F-actin (not shown) indicating that the additional residues from the vector do not bind directly to F-actin. We thus conclude that it is the basic COOH-terminal domain of LSP1, containing a significant homology with the F-actin binding domain of caldesmon, which binds to F-actin.

A quantitative analysis of cosedimentation of rLSP1 with purified F-actin confirms the specificity and high affinity of the LSP1/actin interaction. Fig. 4 *a* shows that the amount of rLSP1 which sediments with F-actin approaches a limiting value near a molar ratio of 1:1 at a 10-fold excess of total LSP1 to sedimented actin. Scatchard analysis of similar data taken from five separate experiments (Fig. 4 *b*) suggests that there is a specific binding interaction with a dissociation constant of ~0.2 μM and an apparent stoichiometry of 0.6 recombinant LSP1 (rLSP1) molecules for each actin subunit. This binding affinity is comparable with that of caldesmon for actin (0.15–0.3 μM) (47). There appears to be a second type of low affinity (apparent $K_d > 5$ μM) interaction that does not approach saturation at the concentrations of rLSP1 that can be achieved experimentally, consistent with the slight increase in binding seen in Fig. 4 *a*. It is not clear

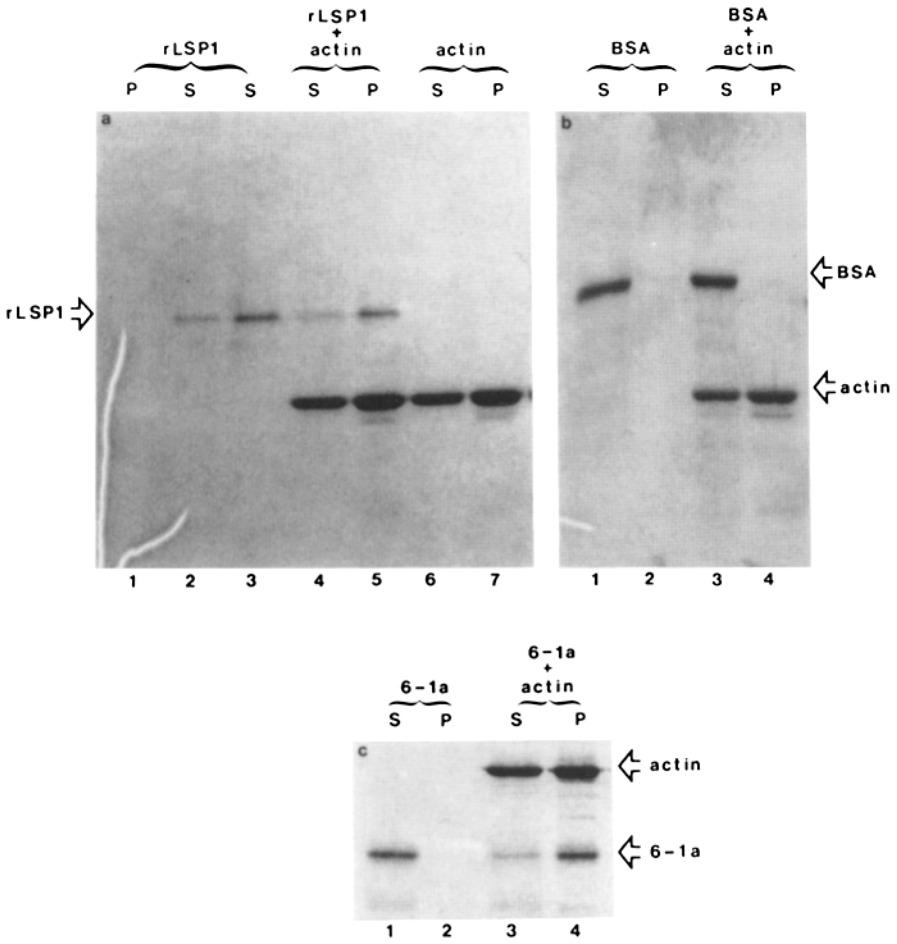

Figure 3. rLSP1 binds to F-actin. F-actin binding assay of rLSP1, BSA and 6-1a analyzed by SDS-PAGE and staining with Coomassie blue. (*a*) rLSP1, 50 μg/ml (lanes *1–3*) or G-actin, 250 μg/ml (lanes *6* and *7*) or both (lanes *4* and *5*) were used for the assay. Half of the pellets (*P*) and the supernatants (*S*) were analyzed except in lanes *2* and *3* which contain 12.5 and 37% of the supernatant, respectively. (*b*) *BSA*, 50 μg/ml (lanes *1* and *2*) or a mixture of the same amount of BSA and G-actin, 250 μg/ml (lanes *3* and *4*) were treated and analyzed as above. (*c*) The 6-1a protein (45 μg/ml) (lanes *1* and *2*) or the same amount of 6-1a with G-actin, 160 μg/ml (lanes *3* and *4*) were used in the assay and one third of the pellets (*P*) and the supernatants (*S*) were analyzed on the gel.

whether the low-affinity binding represents a second F-actin binding site in LSP1 or represents some nonspecific binding or trapping of LSP1 within the actin network during sedimentation. Experiments to map the F-actin binding sites in LSP1 are presently ongoing and should help to resolve this question. The stoichiometry of 0.6 indicated by the Scatchard analysis may be an overestimation since ultrastructural analyses of LSP1/F-actin complexes by EM (see below) revealed the existence of large particles possibly containing several rLSP1 molecules along the sides of the actin filaments. Thus we can not exclude the possibility that this high stoichiometry is due to the presence of nonactin-bound LSP1 molecules associated with actin-bound LSP1.

LSP1 did not greatly affect the rate of actin polymerization. When actin polymerized in solutions containing more than equimolar amounts of LSP1, the initial rate of polymerization, as measured by changes in pyrene fluorescence was the same as that of actin lacking LSP1 (Fig. 5 *a*). At later times, when ~20% of the actin polymerized, the fluorescence increase was slightly retarded by LSP1, but there was no significant effect of a range of LSP1 concentrations on the final fluorescence levels of pyrene-labeled F-actin (data not shown). These results show that LSP1 does not nucleate the formation of actin filaments, which would lead to a large increase in initial rate of polymerization under these conditions, as confirmed by the effect of gelsolin shown in Fig. 5 *a*. LSP1 also does not bind to G-actin with an affinity sufficient to prevent nucleation or the incorporation of monomers into filaments.

In contrast to the lack of effect on the rate of actin polymerization, Fig. 5 *b* shows that rLSP1 augments the light-scattering intensity of F-actin during polymerization. The increased scattering cannot be attributed to additive effects of actin and LSP1 since the latter shows no change in scattering after addition of Mg^{2+} and ATP necessary for actin polymerization. Similar results with fluorescence and light-scattering measurements were obtained when experiments were performed in the presence of NP-40 instead of OGP as detergent. These results, together with the lack of effect on initial fluorescence changes suggest that LSP1 binds actin after its polymerization and forms larger aggregates, possibly by promoting the lateral association of the filaments.

Electron micrographs of F-actin incubated with rLSP1 are strikingly different from actin alone (Fig. 6 *a*). Filaments are bundled and decorated along their sides by small particles of 10–40 nm in diameter (Fig. 6, *b* and *c*). As shown in Fig. 6 *d*, purified specimens of rLSP1 in NP-40 appear as 10–20-nm particles after metal shadowing. These particles were no longer visible by metal shadowing when rLSP1 was preabsorbed onto protein A-Sepharose beads coated with affinity-purified anti-LSP1 antibodies (not shown) indicating that rLSP1 is present in these particles. It is likely therefore that the particles which are intimately associated with actin filaments are the same as those observed in purified rLSP1 sam-

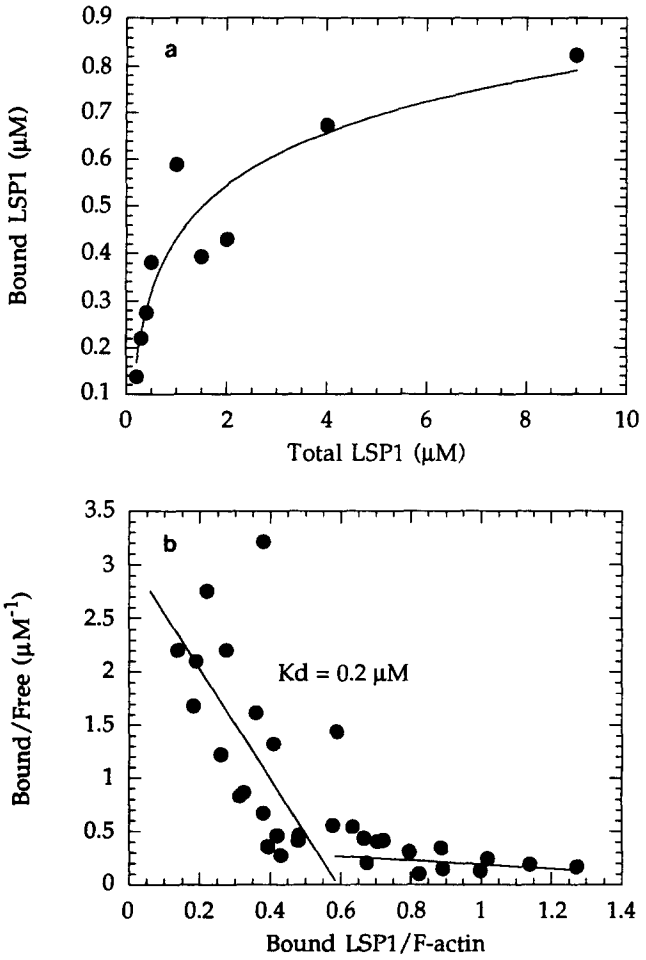

Figure 4. Binding of rLSP1 to F-actin. (*a*) The amount of rLSP1 cosedimenting with F-actin is shown for one series of experiments in which 2 μM G-actin was mixed with various concentrations of LSP1 and then polymerized in 2 mM $MgCl_2$ and 75 mM KCl as described in Materials and Methods. Under these conditions, 0.8 μM F-actin was recovered in the pellet independent of the amount of rLSP1 present. (*b*) Scatchard analysis of several binding experiments using either 2 or 5.9 μM actin. Constant values of 0.8×10^{-10} or 4×10^{-10} moles respectively were used for the sedimented actin. Bound and free LSP1 are expressed as the molar concentrations of LSP1 recovered in the pellet and supernatant, respectively. The line from which an apparent binding affinity is estimated represents a linear least square fit to the binding data for bound LSP1/actin values <0.5.

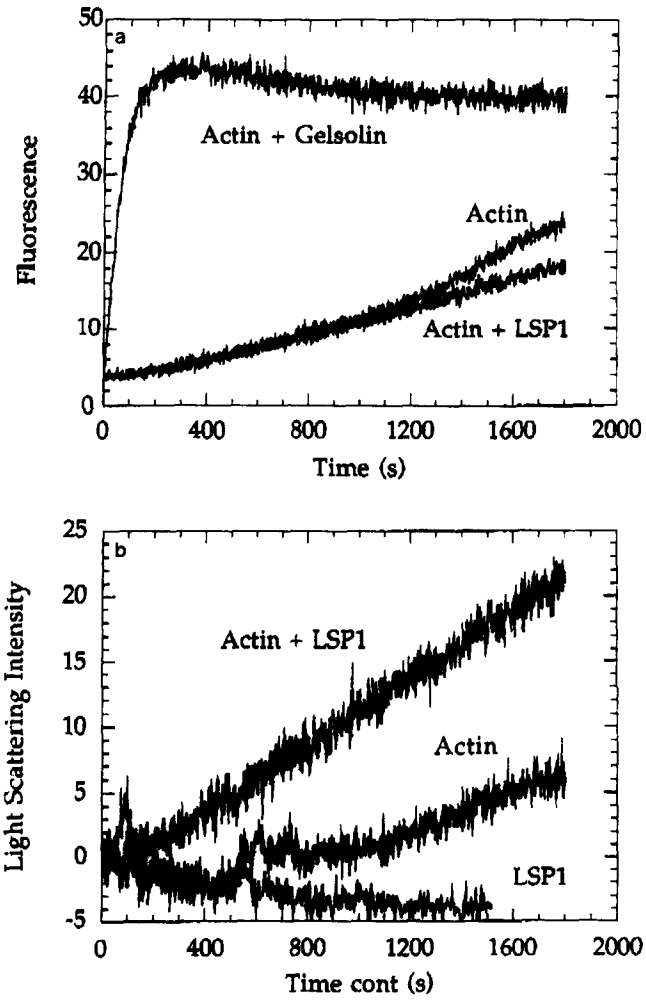

Figure 5. Fluorescence and light scattering measurements. (*a*) Pyrene-labeled actin was polymerized in the presence or absence of LSP1 or gelsolin as described in Materials and Methods. The fluorescence (*a*) and light scattering intensity (*b*) is shown during the initial stage of polymerization in which the pyrene fluorescence of control samples containing only actin reached ~30 % of their final fluorescence levels.

ples. The size of the particles are such that they may contain several LSP1 molecules and the fact that these particles are soluble even after prolonged ultracentrifugation leads us to speculate that the detergent which is necessary to keep rLSP1 soluble may be part of these particles as well. The localization of these particles on actin filaments appears to be dependent on the actin-binding COOH-terminal domain of rLSP1. When F-actin is incubated with rLSP1 the presence of these particles is markedly reduced in regions lacking actin filaments (Fig. 6, *b* and *c*). However, when the truncated LSP1/CAT recombinant fusion protein, 5-1, lacking the COOH-terminal domain and F-actin binding capacity (not shown) is used particles, which also appear in the purified protein specimens (Fig. 6 *f*), are scattered across the grid (Fig. 6 *e*). Furthermore, the 5-1 protein did not aggregate the F-actin filaments. We conclude that the bundling of F-actin filaments by rLSP1 requires the COOH-terminal F-actin binding site of the molecule, since the 5-1 fusion protein does not bind to F-actin nor alters the morphology of the actin filaments (Fig. 6 *e*) as compared with actin alone (Fig. 6 *a*). These observations together with the light scattering experi-

Figure 6. The effects rLSP1 and 5-1 on the ultrastructure of F-actin (*a–c*, and *e*) and the structure of rLSP1 (*d*) and 5-1 (*f*). 3 μM actin was incubated in P buffer without LSP1 (*a*) or with 3 μM LSP1 (*b*), 1.5 μM LSP1 (*c*), or with 3 μM 5-1 (*e*). Actin filaments were visualized by negative staining. (*d* and *f*) 1.5 μM rLSP1 (*d*) and 1.5 μM 5-1 (*f*) were visualized by metal coating. The magnification of all micrographs is identical. Bar, 0.2 μm.

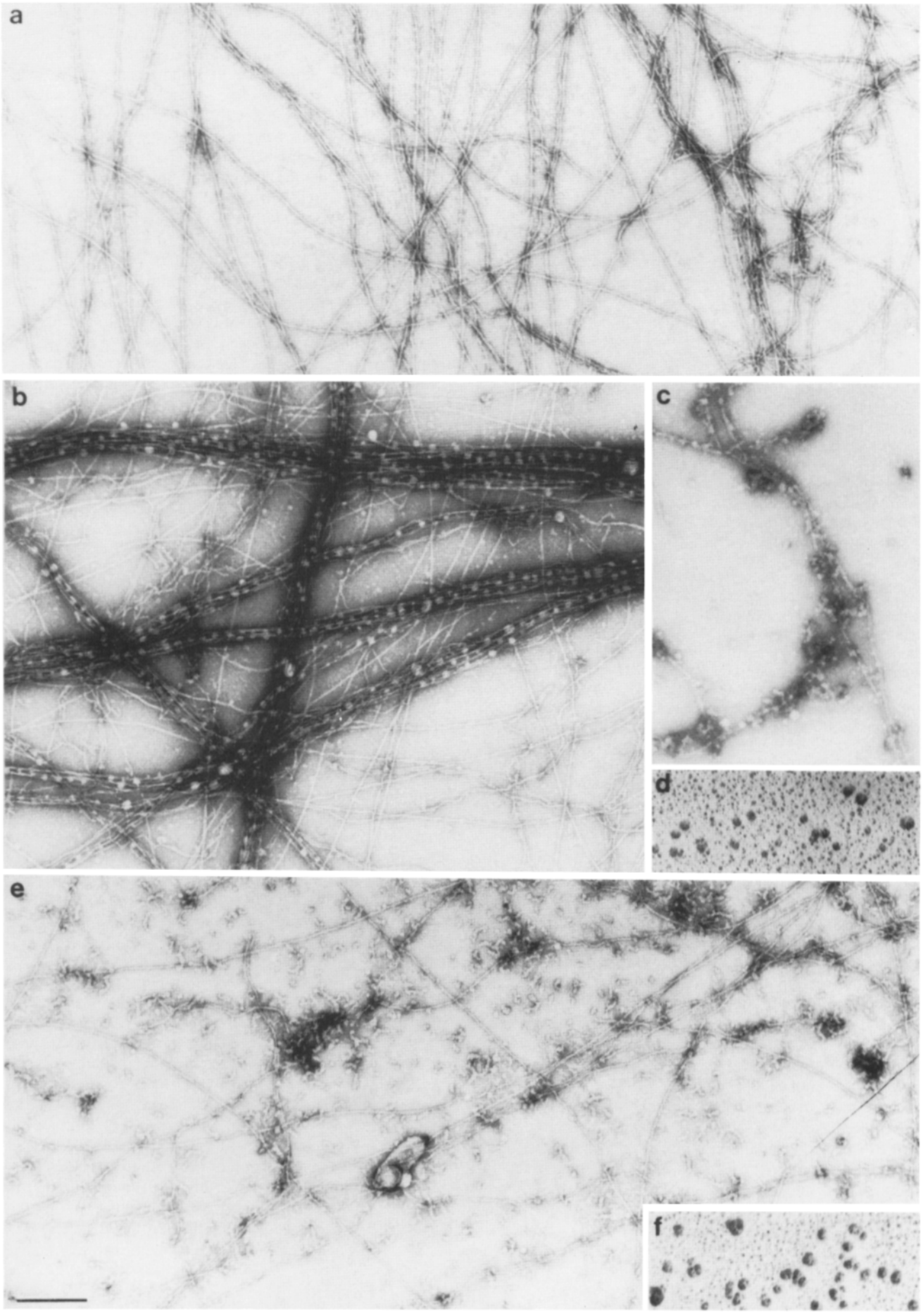
a
b
c
d
e
f

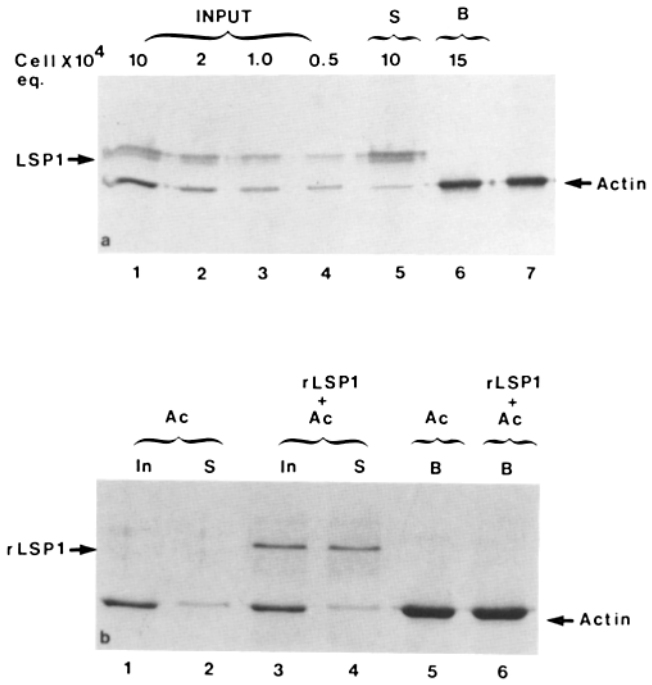

Figure 7. LSP1 does not bind to G-actin. (*a*) Western blot analyses of BAL17 lysates before and after incubation with DNAaseI–Sepharose beads. Material bound to the beads (*B*) and the unbound material in the supernatant (*S*) were analyzed together with different aliquots of the total lysate (*INPUT*) using anti-LSP1 serum (1:2,000) and anti-actin antibodies (1:10) simultaneously. The size of the aliquots is indicated in cell equivalents across the top of the figure. Lane *7* represents 200 ng purified rabbit skeletal muscle actin. (*b*) DNAaseI–Sepharose beads (50 μl 1:1 slurry) were incubated with 20 μg rabbit skeletal muscle G-actin without (lanes *1*, *2*, and *5*) or with 60 μg rLSP1 (lanes *3*, *4*, and *6*) and the beads were spun. Aliquots of the bound (*B*) and the unbound material (*S*) were analyzed together with an aliquot of the input (*In*) on SDS–10% polyacrylamide gels stained with Coomassie brilliant blue. Lanes *1* and *3*, and *2* and *4* represent 1/20th of the input and supernatant, respectively. Lanes *5* and *6* represent one fourth of the bound material.

ments and the stoichiometry of binding lead to the conclusion that binding to F-actin occurs along the sides of the actin filaments.

To determine whether LSP1 binds to G-actin we prepared an NP-40–soluble BAL17 lysate containing the LSP1/actin complex and incubated this lysate with DNAaseI–Sepharose beads. DNAaseI binds with high affinity to G-actin (26, 28) so that if the actin in the LSP1/actin complex in the lysate is G-actin one might expect this complex to be retained on the beads. Fig. 7 *a* shows the result of a typical experiment. The anti-LSP1 serum specifically recognizes a doublet of proteins of a 52-kD LSP1 band and a 50.5-kD as yet uncharacterized band (20). On the blots, the amount of LSP1 and actin present in the different samples was estimated by comparing the LSP1 or actin signal in a sample to the signal present in increasing amounts (expressed as cell equivalents) of the unfractionated lysate used as input (Fig. 7 *a*, lanes *1–4*). Comparison of the actin signals in Fig. 7 *a*, lanes *4* and *5* show that >95% of the actin is removed from the lysate after pelleting the DNAaseI–Sepharose beads. However, essentially all of the LSP1 remains in the lysate. This is also illustrated in Fig. 7 *a*, lane 6 which shows that actin is bound to the beads while no bound LSP1 could be detected, even when five times more beads than shown in Fig. 7 *a*, lane 6 were analyzed (not shown). These results indicate that >95% of the actin present in a NP-40–soluble BAL17 cell lysate is not bound to LSP1.

An alternative explanation of the above results could be that occupation of the LSP1-binding site on G-actin interferes with the binding of G-actin to DNAaseI so that G-actin bound to LSP1 can no longer bind to DNAaseI. To determine whether LSP1 prevents the binding of G-actin to DNAaseI beads we mixed rabbit skeletal muscle G-actin with a threefold excess of rLSP1 before incubating the mixture with DNAaseI–Sepharose beads. Fig. 7 *b*, lanes *5* and *6* demonstrate that the same amount of G-actin binds to the DNAaseI beads regardless of the presence or absence of excess rLSP1 in the incubation mixture. This is also evident from the same observed drop in actin levels between the input and after incubation with the beads when actin is incubated alone (Fig. 7 *b*, lanes *1* and *2*) or with rLSP1 (Fig. 7 *b*, lanes *3* and *4*). Preincubation of G-actin with rLSP1 for 30 min at room temperature before the incubation with the beads gave similar results (not shown). Fig. 7 *b*, lanes *3*, *4*, and *6* also illustrate that rLSP1 does not bind to G-actin bound to DNAaseI beads, which is in accord with the results shown in Fig. 7 *a* using endogenous LSP1 protein from BAL17 lysates. The failure of LSP1 to bind to G-actin agrees with the fact that LSP1 does not affect the rate of actin polymerization.

The Basic Domain of LSP1 Contains a Cytoskeletal Binding Site

Having determined that the basic COOH-terminal half of rLSP1 binds directly to F-actin, we asked whether the same domain directs the protein to the cytoskeleton. To address this question we ligated different parts of the LSP1 cDNA coding sequence upstream of the CAT coding sequence. The resulting constructs were expressed as LSP1/CAT fusion proteins in the LSP1⁻ T-cell line BW5147. Fig. 8 shows the structure of wild-type LSP1 and the different LSP1/CAT proteins used. Five stably transfected cell lines were used: T22, expressing the wild-type LSP1; BW4, expressing a fusion protein consisting of wild-type LSP1 at the NH_2 terminus of the CAT protein (AB-CAT protein); BW57, expressing the acidic LSP1 domain/CAT protein (A-CAT protein); BW71, expressing the basic LSP1 domain/CAT protein (B-CAT protein); and BW711, expressing CAT protein. Fig. 9 represents the distribution of LSP1 and LSP1/CAT fusion proteins in detergent-soluble and insoluble fractions of these cell lines and is representative of several experiments. The percentage of the protein amounts in the detergent-insoluble fractions of these cells illustrated in Fig. 8 were obtained after more extensive titration of the NP-40 insoluble pellets (see Materials and Methods). ~10–20% of wild-type LSP1 is associated with the insoluble fraction in the cell lines WEHI231 and T22 (Fig. 9, *a* and *b*). A similar percentage of AB-CAT protein is also insoluble in BW4 (Fig. 9 *c*) indicating that the presence of the CAT protein COOH terminal to wild-type LSP1 does not significantly influence the distribution of LSP1. As a further control it can be seen that only a small

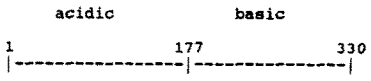

Protein		Cell line	NP-40 Insoluble protein
Wild type	a b	WEHI231	10-20 %
Wild type	a b	T22	10 %
AB-CAT	a b cat	BW4	10 %
A-CAT	a cat	BW57	< 1 %
B-CAT	b cat	BW71	50-100 %
CAT	cat	BW711	< 1 %

Figure 8. Mapping of the cytoskeletal binding domain of LSP1. The top line represents the mouse LSP1 protein and indicates its division in a 177-amino acid long NH_2-terminal acidic domain and a 153-amino acid long COOH-terminal basic domain. The column labeled *Protein* gives the names and schematic representations of the wild-type and fusion proteins used in this study. The column labeled *Cell line* gives the name of the cell line in which the protein is expressed and finally the amount of NP-40 insoluble wild-type or fusion protein is given in the last column.

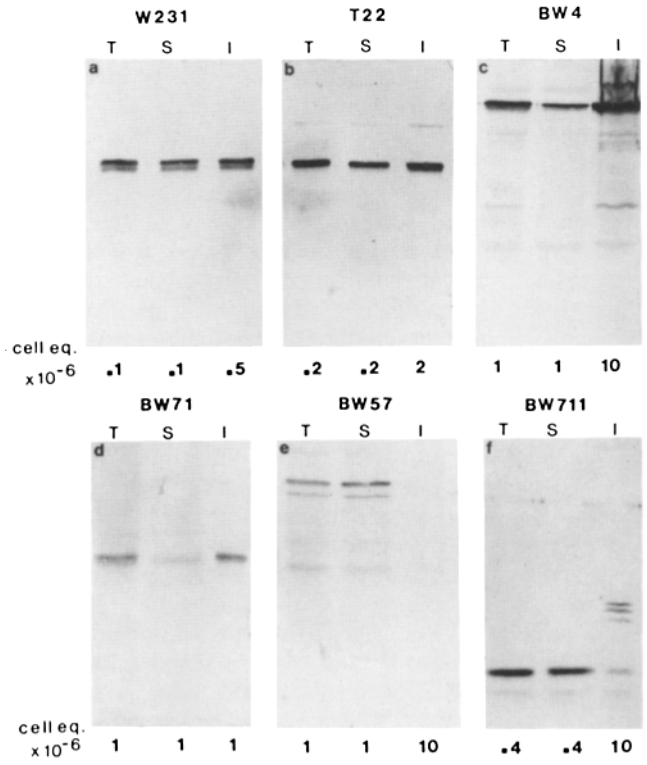

Figure 9. LSP1 binds to the cytoskeleton through its basic domain. Each panel is a Western blot analysis developed using either anti-LSP1 antiserum, 1:2,000 dilution (*a* and *b*) or a mixture of anti-LSP1 and anti-CAT antibodies, 1:2,000 and 1:500 dilutions, respectively (*c*, *d*, and *e*) or anti-CAT antibodies, 1:500 dilution (*f*) and contains a total sample (*T*), a detergent-soluble fraction (*S*), and a detergent-insoluble fraction (*I*) from the cell lines indicated at the top. The size of each sample is indicated in cell equivalents at the bottom of each lane.

percentage (<1%) of CAT protein is insoluble in the cell line BW711 (Fig. 9 *f*). Finally, the majority of the B-CAT protein (50–100%, Fig. 9 *d*) but only a small fraction of the A-CAT protein (<1%, Fig. 9 *e*) is present in the NP-40–insoluble pellets of BW71 and BW57, respectively.

We have previously shown that LSP1 found in the detergent-insoluble fraction of the B-lymphoma cell line BAL17 is associated with the cytoskeleton but not with nuclei which are also present in the detergent-insoluble fraction (21). We verified whether the same is true for the truncated LSP1 fusion protein B-CAT present in the detergent-insoluble fraction of the transfectant line BW71. We prepared a crude lysate of BW71 cells in which the cytoskeletal elements were disrupted but in which the nuclear fraction remained intact using nitrogen cavitation (21) and NP-40 was added to a final concentration of 0.4%, the same final concentration used to lyse whole cells. When this lysate was centrifuged for 10 min at 600 *g* the yield of nuclei was essentially 100%. This was determined by comparing the histone content (as judged from Coomassie blue–stained gels) from equal cell equivalents of the cells before nitrogen cavitation with the NP-40–insoluble pellet. The amount of the B-CAT protein recovered in the detergent-insoluble fraction after nitrogen cavitation was only ~1–5% of the amount found in the crude lysate indicating that the B-CAT protein found in the detergent-insoluble fraction is not associated with the nuclei but rather with the cytoskeleton. These experiments also point out that the presence of high amounts of the B-CAT protein in the detergent-insoluble material is not because of the insolubility of this protein in the NP-40 containing lysis buffer.

The fact that the majority of the B-CAT protein binds to the cytoskeleton is surprising given that the wild-type LSP1 or the AB-CAT protein associates to a much lesser extent with the cytoskeleton. From these results we conclude that it is the actin binding COOH-terminal basic domain of LSP1 which targets LSP1 to the cytoskeleton and that the acidic domain may well play a role in regulating the fraction of total cellular LSP1 protein which binds to the cytoskeleton.

Discussion

The experiments described in this paper show, for the first time, that the lymphocyte-specific protein LSP1 is an F-actin binding protein. The F-actin binding capacity of LSP1 is reproduced with the truncated LSP1 recombinant protein, 6-1a, which contains the entire basic domain of LSP1 but not with another truncated protein, 5-1a, containing only the acidic domain, or with the fusion protein 5-1. Although negative results with the latter two proteins do not exclude the possibility of a folding problem with these recombinant proteins, these results do confirm that the basic domain of LSP1 contains an F-actin binding site. Whether there is more than one actin binding site within this domain or elsewhere in the protein and the exact boundaries of such binding sites are subject for further ongoing studies. The COOH-terminal basic domain of LSP1 which binds to F-actin contains a significant homology with the actin binding domain of caldesmon. Also, the same basic COOH-terminal domain of LSP1 binds directly to the cytoskeleton. These results strongly suggest that the LSP1–F-actin interaction also exists in intact lymphocytes and accounts for the binding of LSP1

to the cytoskeleton. Since the basic COOH-terminal domain of LSP1 is highly conserved between the mouse and human LSP1 proteins (19) this suggests that the F-actin binding capacity of LSP1 is important for its function.

The related 20-kD actin-binding fragment of caldesmon has been reported to bind to calmodulin and it has been proposed that the minimal calmodulin binding site consists of a stretch of seven amino acids from Trp-659 till Ser-666 (41, 44). Although mouse LSP1 protein shares five identical residues with this calmodulin binding site, an interaction between LSP1 and calmodulin was not detected in our immunoprecipitates. Furthermore, preliminary experiments revealed no effect of purified calmodulin on the binding of rLSP1 to F-actin in the presence of Ca^{2+}. These data are consistent with our finding that the interaction of LSP1 with F-actin is not sensitive to Ca^{2+} in cell lysates. Whether other factors such as phosphorylation of LSP1 influences its binding to F-actin remains to be determined.

We showed that LSP1 does not bind to G-actin, which suggests that the actin bound to LSP1 in NP-40–soluble lysates consists of small F-actin oligomers. Fluorescence measurements reveal that LSP1 does not influence the kinetics of actin polymerization, indicating that it is unlikely that LSP1 binds to NP-40–soluble actin oligomers serving as nuclei for actin polymerization (22). Therefore, actin bound to LSP1 in NP-40 lysates most probably represents short actin filaments released during the lysis of cells in NP-40.

EM showed that LSP1 bound to the sides of actin filaments is able to promote bundling of these filaments. Whether bundling is an artifact of the apparent incorporation of rLSP1 into micelles or is of physiological relevance is unknown. Nonmuscle caldesmon bundling of actin filaments has been correlated with the self-association of caldesmon through disulfide bonds (47). Although rLSP1 is not disulfide bonded, it appeared as large 10–20-nm particles in the electron microscope, each possibly containing several rLSP1 molecules and some detergent. The presence of several actin-binding LSP1 molecules in these particles would be expected to promote cross-linking of the actin filaments to form bundles.

It has become apparent that the lymphocyte cytoskeleton plays an important role in lymphocyte activation. Two series of experiments with sets of monoclonal anti-IgM or anti-IgD antibodies showed a strict correlation between the capacity of the antibodies to induce capping and their ability to induce the attachment of mIg to the cytoskeleton or to induce a mitogenic response in B-lymphocytes (1, 14). In addition Melamed et al. (29) showed that blocking the anti-Ig induced F-actin assembly by treatment with cytochalasin D or botulinum C2 toxin prevented subsequent DNA synthesis. The block in DNA synthesis appeared to be distal to activation of protein kinase c since treatment with botulinum C2 also blocked phorbol ester–induced F-actin assembly and DNA synthesis. These results imply a role for the cytoskeleton in the early and late stages of the transduction of anti-Ig generated signals. LSP1 could be involved in several aspects of this signal transduction process, for instance in the cytoskeleton-mediated capping of surface antigen receptors on B- and T-lymphocytes or in the anti-Ig–induced association of mIg molecules with the cytoskeleton. The molecular nature of the linkage between mIg and the cytoskeleton is unclear. It has been postulated that mIg binds directly to actin (11), or that specific proteins such as Gc globulin (35) or α-actinin (15) are involved. However, it is possible that LSP1 plays a role in this process, possibly by binding directly to mIg or to the recently described Ig-associated proteins (7, 16). Other roles for LSP1 can, however, not be excluded. The cytoskeleton participates in the proper functioning of the immune system through its involvement in important processes such as adhesion of lymphocytes to the specialized high endothelial venules (HEV) which is the first step in the extravasation process by which lymphocytes leave the blood stream to enter secondary lymphoid organs such as lymph nodes (46). The cytoskeleton must also play a role in regulating the dramatic shape changes which lymphocytes must undergo when passing between endothelial cells (2). Furthermore, it has been shown that the cytoskeleton plays a role in the interactions between helper T-cells and antigen presenting B-cells (23, 24) or between cytotoxic T-cells and their targets (13, 33). Since LSP1 is present at the strategic interface of the plasma membrane with the cell cytoplasm, possibly as part of the membrane skeleton, this localization may allow LSP1 to transmit signals from the lymphocyte membrane to the cytoskeleton mediating any of the cytoskeleton-driven responses discussed above.

We thank Dr. Dominique Aunis for his generous gift of the anti-actin antibodies, Dr. Steve Kron for his advice and generous gift of actin at the early stages of this work, and Dr. Owen Jones for helpful discussions. We also thank Nicole King-Trickey, Jennifer Lamb, and John Kim for excellent technical help.

This work was supported by grants to J. Jongstra from the Medical Research Council of Canada and the National Cancer Institute of Canada and from the National Institutes of Health to P. A. Janmey (AR38910) and J. H. Hartwig (HL47874). J. Jongstra is a Scholar of the McLaughlin Foundation and J. Jongstra-Bilen is the recipient of a fellowship award from the Leukemia Society of America, Inc.

Received for publication 14 January 1992 and in revised form 5 May 1992.

References

1. Albrecht, D. L., and R. J. Noelle. 1988. Membrane Ig-cytoskeletal interactions. I. Flow cytofluorometric and biochemical analysis of membrane IgM-cytoskeletal interactions. *J. Immunol.* 141:3915–3922.
2. Anderson, A. O., and N. D. Anderson. 1976. Lymphocyte emigration from high endothelial venules in rat lymph nodes. *Immunology.* 31:731–748.
3. Bijsterbosch, M. K., C. J. Meade, G. A. Turner, and G. G. B. Klaus. 1985. B-lymphocyte receptors and polyphosphoinositide degradation. *Cell.* 41:999–1006.
4. Braun, J., and E. R. Unanue. 1980. B lymphocyte biology studied with anti-Ig antibodies. *Immunol. Rev.* 52:3–28.
5. Braun, J., P. S. Hochman, and E. R. Unanue. 1982. Ligand-induced association of surface immunoglobulin with the detergent-insoluble cytoskeletal matrix of the B lymphocyte. *J. Immunol.* 128:1198–1204.
6. Bryan, J., M. Imai, R. Lee, P. Moore, R. G. Cook, and W.-G. Lin. 1989. Cloning and expression of a smooth muscle caldesmon. *J. Biol. Chem.* 264:13873–13879.
7. Campbell, K. S., and J. C. Cambier. 1990. B lymphocyte antigen receptors (mIg) are non-covalently associated with a disulfide linked, inducibly phosphorylated glycoprotein complex. *EMBO (Eur. Mol. Biol. Organ.) J.* 9:441–448.
8. Campbell, M.-A., and B. M. Sefton. 1990. Protein tyrosine phosphorylation is induced in murine B lymphocytes in response to stimulation with anti-immunoglobulin. *EMBO (Eur. Mol. Biol. Organ.) J.* 9:2125–2131.
9. Coggeshall, K. M., and J. C. Cambier. 1984. B cell activation. VIII. Membrane immunoglobulins transduce signals via activation of phosphatidylinositol hydrolysis. *J. Immunol.* 133:3382–3386.
10. DeFranco, A. L., E. S. Raveche, R. Asofsky, and W. E. Paul. 1982. Frequency of B lymphocytes responsive to anti-immunoglobulin. *J. Exp. Med.* 155:1523–1536.
11. Flanagan, J., and G. L. E. Koch. 1978. Cross-linked surface Ig attaches to actin. *Nature (Lond.).* 273:278–281.
12. Gold, M. R., D. A. Law, and A. L. DeFranco. 1990. Stimulation of protein

tyrosine phosphorylation by the B-lymphocyte antigen receptor. *Nature (Lond.).* 345:810–813.
13. Golstein, P., C. Foa, and I. C. M. MacLennan. 1978. Mechanism of T cell mediated cytolysis: the differential impact of cytochalasins at the recognition and lethal hit stages. *Eur. J. Immunol.* 8:302–309.
14. Goroff, D. K., A. Stall, J. J. Mond, and F. D. Finkelman. 1986. In vitro and in vivo B lymphocyte-activating properties of monoclonal anti-delta antibodies. I. Determinants of B lymphocyte-activating properties. *J. Immunol.* 136:2382–2392.
15. Gupta, S. K., and B. A. Woda. 1988. Ligand-induced association of surface immunoglobulin with the detergent insoluble cytoskeleton may involve alpha-actinin. *J. Immunol.* 140:176–182.
16. Hombach, J., T. Tsubata, L. Leclercq, H. Stappert, and M. Reth. 1990. Molecular components of the B-cell antigen receptor complex of the IgM class. *Nature (Lond.).* 343:760–762.
17. Howard, M., J. Farrar, M. Hilfiker, B. Johnson, K. Takatsu, and W. E. Paul. 1982. Identification of a T-cell–derived B cell growth factor distinct from interleukin 2. *J. Exp. Med.* 155:914–923.
18. Jongstra, J., G. F. Tidmarsh, J. Jongstra-Bilen, and M. M. Davis. 1988. A new lymphocyte-specific gene which encodes a putative Ca^{2+}-binding protein is not expressed in transformed T lymphocyte lines. *J. Immunol.* 141:3999–4004.
19. Jongstra-Bilen, J., A. J. Young, R. Chong, and J. Jongstra. 1990. Human and mouse LSP1 genes code for highly conserved phosphoproteins. *J. Immunol.* 144:1104–1110.
20. Klein, D. P., J. Jongstra-Bilen, K. Ogryzlo, R. Chong, and J. Jongstra. 1989. Lymphocyte-specific Ca^{2+}-binding protein LSP1 is associated with the cytoplasmic face of the plasma membrane. *Mol. Cell. Biol.* 9:3043–3048.
21. Klein, D. P., S. Galea, and J. Jongstra. 1990. The lymphocyte-specific protein LSP1 is associated with the cytoskeleton and co-caps with membrane IgM. *J. Immunol.* 145:2967–2973.
22. Korn, E. D. 1982. Actin polymerization and its regulation by proteins from non muscle cells. *Physiol. Rev.* 62:672–737.
23. Kupfer, A., and S. J. Singer. 1989. The specific interaction of helper T cells and antigen-presenting B cells. IV. Membrane and cytoskeletal reorganizations in the bound T cell as a function of antigen dose. *J. Exp. Med.* 170:1697–1713.
24. Kupfer, A., S. Swain, and S. J. Singer. 1987. The specific interaction of helper T cells and antigen-presenting B cells. II. Reorganization of the microtubule organizing center and reorganization of the membrane-associated cytoskeleton inside the bound helper T cells. *J. Exp. Med.* 165:1565–1580.
25. Laemmli, U. K. 1970. Cleavage of structural proteins during the assembly of the head of bacteriophage T4. *Nature (Lond.).* 227:680–685.
26. Lazarides, E., and U. Lindberg. 1974. Actin is the naturally occuring inhibitor of deoxyribonuclease I. *Proc. Natl. Acad. Sci. USA.* 71:4742–4746.
27. Lin, A. Y., B. Devaux, A. Green, C. Sagerstroem, J. F. Elliott, and M. M. Davis. 1990. Expression of T cell antigen receptor heterodimers in a lipid-linked form. *Science (Wash. DC).* 249:677–679.
28. Mannherz, H. G., R. S. Goody, M. Konrad, and E. Nowak. 1980. The interaction of bovine pancreatic deoxyribonuclease I and skeletal muscle actin. *Eur. J. Biochem.* 104:367–379.
29. Melamed, I., G. P. Downey, and C. M. Roifman. 1991. Microfilament assembly is required for antigen receptor mediated activation of human B-lymphocytes. *J. Immunol.* 147:1139–1146.
30. Misener, V., J. Jongstra-Bilen, A. J. Young, M. J. Atkinson, G. E. Wu, and J. Jongstra. 1990. Association of Ig L chain-like protein lambda5 with a 16-kilodalton protein in mouse pre-B cell lines is not dependent on the presence of Ig H chain protein. *J. Immunol.* 145:905–909.
31. Myers, C. D., M. K. Kritz, T. J. Sullivan, and E. S. Vitetta. 1987. Antigen-induced changes in phospholipid metabolism in antigen-binding B lymphocytes. *J. Immunol.* 138:1705–1711.
32. Nel, A. E., G. E. Landreth, P. J. Goldschmidt-Clermont, M. E. Tung, and R. M. Galbraith. 1984. Enhanced tyrosine phosphorylation in B lymphocytes upon complexing of membrane immunoglobulin. *Biochem. Biophys. Res. Commun.* 125:859–866.
33. O'Rourke, A. M., J. R. Apgar, K. P. Kane, E. Martz, and M. F. Mescher. 1991. Cytoskeletal function in CD8- and T cell receptor-mediated interaction of cytotoxic T lymphocytes with Class I protein. *J. Exp. Med.* 173:241–249.
34. Osborn, M., and K. Weber. 1977. The detergent-resistant cytoskeleton of tissue culture cells includes the nucleus and the microfilament bundles. *Exp. Cell Res.* 106:339–347.
35. Petrini, M., D. L. Emerson, and R. M. Galbraith. 1983. Linkage between surface immunoglobulin and cytoskeleton of B lymphocytes may involve Gc protein. *Nature (Lond.).* 306:73–74.
36. Pozzan, T., P. Arslan, R. Y. Chien, and T. J. Rink. 1982. Anti-immunoglobulin, cytoplasmic free calcium, and capping in B lymphocytes. *J. Cell Biol.* 94:335–340.
37. Ransom, J. T., L. K. Harris, and J. C. Cambier. 1986. Anti-Ig induces release of inositol 1,4,5-trisphosphate, which mediates mobilization of intracellular Ca^{2+} stores in B lymphocytes. *J. Immunol.* 137:708–714.
38. Rothstein, T. L. 1986. Stimulation of B cells by sequential addition of anti-immunoglobulin antibody and cytochalasin. *J. Immunol.* 136:813–816.
39. Schreiner, G. F., and E. R. Unanue. 1975. Anti-Ig triggered movements of lymphocytes-specificity and lack of evidence for directional migration. *J. Immunol.* 114:809–814.
40. Sieckmann, D. G., R. Asofsky, D. E. Mosier, I. A. Zitron, and W. E. Paul. 1978. Activation of mouse lymphocytes by anti-immunoglobulin. I. Parameters of the proliferative response. *J. Exp. Med.* 147:814–829.
41. Sobue, K., and J. R. Sellers. 1991. Caldesmon, a novel regulatory protein in smooth muscle and nonmuscle actomyosin systems. *J. Biol. Chem.* 266:12115–12118.
42. Spudich, J. A., and S. Watt. 1971. The regulation of rabbit skeletal muscle contraction: biochemical studies of the interaction of the tropomyosin-troponin complex with actin and the proteolytic fragments of myosin. *J. Biol. Chem.* 246:4866–4871.
43. Tyler, J. M., J. M. Anderson, and D. Branton. 1980. Structural comparison of several actin binding molecules. *J. Cell Biol.* 85:489–495.
44. Wang, C.-L. A., L.-W. C. Wang, S. Xu, R. C. Lu, V. Saavedra-Alanis, and J. Bryan. 1991. Localization of the calmodulin- and actin-binding sites of caldesmon. *J. Biol. Chem.* 266:9166–9172.
45. Woda, B. A., and M. B. Woodin. 1984. The interaction of lymphocyte membrane proteins with the lymphocyte cytoskeletal matrix. *J. Immunol.* 133:2767–2772.
46. Woodruff, J. J., I. M. Katz, L. E. Lucas, and H. B. Stamper, Jr. 1977. An in vitro model of lymphocyte homing. II. Membrane and cytoplasmic events involved in lymphocyte adherence to specialized high-endothelial venules of lymph nodes. *J. Immunol.* 119:1603–1610.
47. Yamashiro-Matsumura, S., and F. Matsumura. 1988. Characterization of 83-kilodalton nonmuscle caldesmon from cultured rat cells: stimulation of actin binding of nonmuscle tropomyosin and periodic localization along microfilaments like tropomyosin. *J. Cell Biol.* 106:1973–1983.